Bio-Medical Materials and Engineering 24 (2014) 3321–3332
DOI 10.3233/BME-141155
IOS Press

Level set model with local fitting operation of median filter

Xi Liu and Lixiong Liu*
Beijing Laboratory of Intelligent Information Technology, School of Computer Science and Technology, Beijing Institute of Technology, Beijing 100081, China

Abstract. We analyzed the principle of the traditional local binary fitting operation, Gaussian kernel function weighted summation (GKFWS), to develop a novel level set model in this paper. In this model, the traditional GKFWS operation is replaced with the median filter operation in the second procedure of local fitting of the energy domain. Furthermore, we incorporated the edge stopping function of GAC model into it to introduce the edge information for segmentation. Experiments on synthetic and real images demonstrate that this model has promising performance in terms of computational cost, robustness to noises and segmentation of images with intensity inhomogeneity.

Keywords: Active contour, median filter, image segmentation, level set, edge information

1. Introduction

During the past few decades, medical image segmentation has been an area of hot research in the field of image processing. In recent years, a variety of ideas concerning this field has been proposed, including region competition algorithms to deal with sonography segmentation [1,2], algorithms based on Fuzzy C-Mean clustering, segmentation methods based on Wavelet Transform, novel models with the shape prior information, and so on. Among all these methods, active contours or snakes have been the most prevalent and influential variational image segmentation method since its introduction [3] in 1987. Snakes are contours that could conform to object boundaries or other image features under the attractions of internal and external forces from the image data. Generally, snakes can be classified as parametric snakes [4,5] requiring an explicit representation or as geometric snakes [6] defined as a curve implicitly. Compared with parametric snakes, geometric snakes or level set models are more robust to contour initialization and able to handle the topology changes of contours automatically. This paper concentrates on an improved novel geometric snake. The existing geometric snakes can be classified as edge-based and region-based models. Geodesic active contour is the first edge-based level set model which conforms to the object boundaries according to edge information of the image [7]. It can segment images with obvious edge feature successfully and split into several target regions automatically. However, edge-based models are all unable to process images without obvious edge information and are very sensitive to contour initialization. Chan-Vese (CV) model [8] is one of the

*Corresponding author: Lixiong Liu, School of Computer Science and Technology, Beijing Institute of Technology, Beijing 100081, China. Tel.: +86 01068913475; E-mail: lxliu@bit.edu.cn.

most popular region-based level set models. This model can be successfully applied to simple images with two homogeneous regions, each represented by a distinct mean of pixel intensity. And it can distinguish multiple target regions with weak edges using the statistical information of the different regions. However, CV model is not capable of segmenting the inhomogeneous or high-level-noise images because of its requirement for statistical homogeneity for the different regions. Li et al. proposed a new region-based model called Local Binary Fitting (LBF) model [9] which overcomes these problems to a certain extent. The key difference between the two models is that the CV model takes single global means of pixel intensity to fit the regions which only can be right for the homogenous images, while LBF model fit every single pixel's value according to its neighborhood intensity distribution which introduces local property for segmentation.

Since then, there are many efficient region-based models due to the success of LBF's local fitting. Wang et al. proposed a novel model based on dual contour evolutional curve [10]. Wang et al. proposed the LCV model [11] capable of segmenting inhomogeneous images by embedding a differential image fitting term into the CV formulation. Liu et al. proposed a novel model [12] which combines the global property of CV and local property of LBF with the intensity inhomogeneity theory. Wang et al. proposed a local and global intensity linear fitting model to solve the LBF's problem of sensitivity to curve initialization [13]. Zhang et al. took the mean of global region intensity into consideration, as proposed in their LIF model [14].

Among all above models, their ideas focus on either the problem of curve initialization or proposing a new form to fit image and embedding a new energy term into the original energy formulation. They all calculated the results with the traditional Gaussian Kernel Function Weighted Summation (GKFWS) [9] when fitting the pixel intensity values and energy terms. However, in some cases this kind of weighted summation operation can lead to excessive smoothing of the edge features of the image (while better than CV model which has no edge features inside one region). On the other hand, it would inevitably introduce more noise influences into the results for images contaminated with high levels of noise. As a result, these two problems constrain the application of these models. Fortunately, Reddy et al. proposed a quick bit plane techniques to implement median functions in the binary domain and embed the median filtered image information in the edge stopping function of the geodesic active contour [7], this ensured noise robustness for segmenting images with high levels of noise [15]. Whereas this model still requires the obvious edge feature to get the correct results and is very sensitive to contour initialization. Based on these previous studies [9,15], we propose a novel region-based level set model which replaces the GKFWS with the median filter operation and introduces the energy term of edge information.

This paper is organized as follows. In Section 2, we review the classic region-based and edge-based models. Section 3 defines our fitting operation of median filter and the energy term and describes how to construct the energy functional formulation in our model. The performance of our model is demonstrated in section 4. Finally, we summarize our findings in section 5.

2. Background

2.1. CV model

Chan and Vese proposed CV model [8] as a particular case of Mumford-Shah model [16]. It hypothesizes that the image consists of two regions of approximately piecewise-constant intensities. So the model could fit the piecewise-constant intensities for the simple images formed by regions

between which there are distinct intensity values *c1* and *c2*. For an image *I(x)*, we could obtain the energy functional defined by:

$$E^{CV}(C,c_1,c_2)=\lambda_1 \int_{in(C)}|I(x)-c_1|^2dx+\lambda_2 \int_{out(C)}|I(x)-c_2|^2dx+v|C|. \quad (1)$$

where *in(C)* denotes the inner region of the contour *C*, *out(C)* denotes the outer region of the contour *C, c1* and *c2* represent the means of pixel intensities in *in(C)* and *out(C)* respectively. *I(x)* is the intensity of the pixel in *x*. We call the first two terms the global binary fitting energy term. Clearly, minimization of the energy functional could only be implemented when the mean intensities of the two regions are close to the corresponding pixel intensities. The third term is the length energy term constraining the length and smoothness of the contour. The energy functional can be transformed into a level set evolution equation which can be solved by the level set method.

In Eq. (1), *c1* and *c2* represent the fitting value (mean intensity) of the inner region and outer region respectively. Clearly, due to contamination of noises or intensity inhomogeneity, global fitting values such as the mean intensities are not representative of the regions' features when the insides of the two regions are heterogeneous. So CV model can segment only the images that contain simple foreground and background regions, and would fail to segment the images with heterogeneous regions.

2.2. LBF model

To solve the segmentation capacity limitation of CV model, Li et al. proposed Local Binary Fitting (LBF) model which introduces the local property of the image [9]. The energy functional of the LBF model is defined by:

$$E^{LBF}=\lambda_1 \int_{in(C)} K_\sigma(|x-y|)|I(y)-f_1(x)|^2dxdy+\lambda_2 \int_{out(C)} K_\sigma(|x-y|)|I(y)-f_2(x)|^2dxdy, \quad (2)$$

where *f1(x)* and *f2(x)* are the binary fitting functions that replace the constant functions *c1*, *c2* in the CV model, and K_σ is the Gaussian kernel function with scale parameter $\sigma > 0$. Point *x* is the center point of the neighborhood and *y* is a point in the neighborhood of *x*. The Gaussian kernel function has a localization property that $K_\sigma(|x-y|)$ gradually decreases and approaches zero as $|x-y|$ increases. That means the energy functional would be more influential near the center point and less influential away from it. The local fitting functions *f1(x)* and *f2(x)* fit the image pixel intensity according to the intensities of neighborhood near *x* with the same localization property provided by Gaussian kernel function $K_\sigma(|x-y|)$. Eqs. (3) and (4) are the calculation equations of *f1(x)* and *f2(x)*:

$$f_1(x)=\frac{K_\sigma(x)*[H_\varepsilon(\phi(x))I(x)]}{K_\sigma(x)*[H_\varepsilon(\phi(x))]}, \quad (3)$$

$$f_2(x)=\frac{K_\sigma(x)*[(1-H_\varepsilon(\phi(x)))I(x)]}{K_\sigma(x)*[1-H_\varepsilon(\phi(x))]}, \quad (4)$$

where H_ε is a smooth function that approximates the Heaviside function H for the stability of numerical calculation. The Heaviside function is used to label different regions by $H=1$ in inner region and $H=0$ in outer region. Function H_ε and its derivative are defined by Eqs. (5) and (6):

$$H_\varepsilon(x)=\frac{1}{2}\left[1+\frac{2}{\pi}arctan\left(\frac{x}{\varepsilon}\right)\right], \tag{5}$$

$$\delta_\varepsilon(x)=H'(x)=\frac{1}{\pi}\frac{\varepsilon}{\varepsilon^2+x^2}. \tag{6}$$

By introducing the Heaviside function, we could transform Eq. (5) into Eq. (7):

$$E^{LBF}(f_1,f_2,\phi)=\mu P(\phi)+\nu L(\phi)+\lambda_1\int\left[\int K_\sigma(|y-x|)\left|I(y)-f_1(x)\right|^2 H_\varepsilon(\phi(y))dy\right]dx$$
$$+\lambda_2\int\left[\int K_\sigma(|y-x|)\left|I(y)-f_2(x)\right|^2\left(1-H_\varepsilon(\phi(y))\right)dy\right]dx. \tag{7}$$

For the stability of numerical implementation of level set evolution, the penalization energy term $P(\phi)$ in [17] is introduced. It could penalize the deviation of the level set function from a signed distance function. This deviation of the level set function from a signed distance function is defined by the following integral functional:

$$\mathrm{P}(\phi)=\int_\Omega\frac{1}{2}\left(|\nabla\phi(x)|-1\right)^2dx, \tag{8}$$

To normalize the zero level contour of the level set function ϕ, it is necessary to consider the length of the zero level curve of ϕ, which is defined by:

$$\mathrm{L}(\phi)=\int_\Omega\delta(\phi(x))|\nabla\phi(x)|dx, \tag{9}$$

Using the standard gradient descent method to minimize the energy functional, we can deduce its gradient descent flow:

$$\frac{\partial\phi}{\partial t}=-\delta_\varepsilon(\phi)\left(\lambda_1e_1-\lambda_2e_2\right)+\nu\delta_\varepsilon(\phi)div\left(\frac{\nabla\phi}{|\nabla\phi|}\right)+\mu\left(\nabla^2\phi-div\left(\frac{\nabla\phi}{|\nabla\phi|}\right)\right), \tag{10}$$

where e1 and e2 are defined by Eqs. (11) and (12), respectively:

$$e_1=\int_\Omega K_\sigma(y-x)\left|I(x)-f_1(y)\right|^2dy, \tag{11}$$

$$e_2=\int_\Omega K_\sigma(y-x)\left|I(x)-f_2(y)\right|^2dy. \tag{12}$$

Compared with CV model, LBF model uses fitting functions *f1(x)* and *f2(x)* to fit the image intensities according to the center points' neighborhoods. This introduces the local property into the fitting functions *f1(x)* and *f2(x)* whereas CV model's global constant functions *c1* and *c2* only accounts for global property. As a result, LBF model has the ability to segment images with heterogeneous regions.

2.3. GAC model

Casseles et al. proposed Geodesic Active Contour (GAC) model [7] which is the first edge-based geometric active contour model. Given an image *I*, *C(q)* is the parametric curve in the image domain, the model's energy functional is defined by:

$$E^{GAC}(C)=\int_0^1 g\left(\left|\nabla I(C(q))\right|\right)\left|C'(q)\right|dq, \tag{13}$$

where *g* denotes the edge stopping function:

$$g(|\nabla I|)=\frac{1}{1+|\nabla G_\sigma * I|^2} \tag{14}$$

The edge stopping function has following two major properties. First, $|\nabla I|$ would get larger in the regions of image edge. Second, it would get values close to 0 in the homogeneous regions. Thus *g* is to stop the evolving curve as it conforms to the objects boundaries. The gradient descent flow of Eq. (13) is defined by Eq. (15):

$$\frac{\partial \phi}{\partial t}=g(|\nabla \phi|)\left(div\left(\frac{\nabla \phi}{|\nabla \phi|}\right)+\alpha\right)+\nabla g\cdot\nabla \phi. \tag{15}$$

3. Our model

3.1. Fitting operation of median filter and edge energy term

In LBF model, there are two procedures of GKFWS for local fitting. The first procedure fits the pixel intensity values of the fitting image, and the second one fits the fitting energy of the energy domain. Both of them make use of the GKFWS that introduces local property into the model such that the LBF model could segment images with heterogeneous regions. However, these two fitting procedures can lead to two major problems. First, when the image is contaminated heavily by noise, the intensity fitting image would inevitably be influenced by so much noise that it probably gives an incorrect segmentation result. Second, the simple GKFWS would probably smooth the edge information too much to keep proper edge feature. In order to overcome these two side effects, we replaced the GKFWS with the median filter operation. The median filter is a nonlinear digital filtering technique often used to effectively remove noise in images or other signals. It is able to maintain the original edge information while effectively removing noises such as speckle noises, pepper and salt noises and so on [15,18,19]. Therefore with the process of median filter operation, our model can keep

more of the original edge information. At the same time, as the LBF model is a region-based model which does not introduce any edge information in the segmentation process, it may fail to segment some images because of the absence of edge information. Thus, we introduced the GAC model's edge stopping function energy term into our model to make use of the edge information.

In general, the median filter, as a nonlinear digital filter, exhibits slower speed of calculation than the GKFWS in the same neighborhood with traditional method of calculation. However, Reddy et al. proposed novel bit plane techniques to implement median functions in the binary domain [15], which can drastically reduce the computational cost of noise removal by implementing the calculation with FPGAs. So we adopted the iteration number as the basic unit of computational cost and ignored the basic time consumption of a single calculation.

The model in [15] also incorporated the median filter operation into its energy functional. However, Reddy's model is an improved edge-based model by refining the static edge information which never changes in the segmentation process, whereas our model is an improved region-based model by refining the dynamic region information which is always updated in the segmentation process. Therefore, our model represents a different way of introducing the median filter operation into a novel model with the major idea shown in [15].

3.2. Variational level set formulation of our model

We represented the evolution curve of the model with level set function ϕ and replaced the GKFWS with median filter operation. Thus, we can define the new energy functional by Eq. (16):

$$\begin{aligned} F^{New} &= E_{new}(f_1, f_2, \phi) + \alpha G(\phi) + \mu P(\phi) + \nu L(\phi) \\ &= \iint_{\Omega} \left[\lambda_1 Med\left(\left| I(y) - f_1(x) \right|^2 \right) H_\varepsilon(\phi(y)) + \lambda_2 Med\left(\left| I(y) - f_2(x) \right|^2 \right) \left(1 - H_\varepsilon(\phi(y)) \right) \right] dydx \\ &\quad + \alpha G(\phi) + \mu P(\phi) + \nu L(\phi) \end{aligned} \tag{16}$$

where *Med(.)* denotes the median filter operation to the image energy domain, E_{new} represents the differential energy term between the local fitting functions *f1(x)*, *f2(x)* and the original image. The GKFWS in the LBF model has been replaced with the median filter operation *Med(.)* which is more robust at removing noises and better at keeping the original edge information [18,19]. $G(\phi)$ is the edge stopping function energy term containing edge information of the image. $P(\phi)$ is the penalization energy term used to penalize the deviation of the level set from the signed distance function. $L(\phi)$ is the length energy term used to control the degree of the contour's smoothness. $\lambda_1, \lambda_2, \alpha, \mu$ and ν are constant parameters that control the influences of the corresponding energy terms respectively.

Of note, we replaced the GKFWS with the median filter operation in the procedure for energy domain fitting rather than image domain fitting. This is because in the procedure of image domain fitting, the model would get a basic differential energy by subtracting the fitting image from the original image. This basic differential energy plays a crucial role in the subsequent segmentation process. After experimental validations, we found that the basic differential energy calculated by traditional GKFWS is much smaller than the median filter operation. Thus, it may lead to incorrect segmentation results because of the excessive modification by using the median filter operation in this fitting procedure. At the same time, the procedure of energy domain fitting based on previous differential energy could use the median filter operation and would not lead to an excessive reduction

in differential energy. Furthermore, the result of the energy domain fitting would feedback to the procedure of image domain fitting in return, which can improve its robustness to the noise and ability to keep the original edge information.

The gradient descent flow equation of the energy functional (16) is defined by:

$$\frac{\partial \phi}{\partial t} = -\delta_\varepsilon(\phi)\left(\lambda_1 e_1 - \lambda_2 e_2\right) + \nu\delta_\varepsilon(\phi)\,div\left(\frac{\nabla\phi}{|\nabla\phi|}\right) + \mu\left(\nabla^2\phi - div\left(\frac{\nabla\phi}{|\nabla\phi|}\right)\right) + \alpha\delta_\varepsilon(\phi)\,div\left(g\frac{\nabla\phi}{|\nabla\phi|}\right), \tag{17}$$

where e_1, e_2 are given by

$$e_1 = \int_\Omega Med\left(\left|I(x) - f_1(y)\right|^2\right) dy, \tag{18}$$

$$e_2 = \int_\Omega Med\left(\left|I(x) - f_2(y)\right|^2\right) dy. \tag{19}$$

4. Experiments and analysis

The following experiments were performed on synthetic and real images under a Lenovo desktop computer with the Intel core CPU, 3.2 GHz and 8 GB RAM. The comparison with three models illustrates the promising performance of our model in terms of computational cost, robustness to noise and segmentation of images with intensity inhomogeneity.

For the convenience of comparing the computational cost of these three models, Table 1 shows all the iteration numbers of the three models in the following five experiments.

4.1. Synthetic images with intensity inhomogeneity/ high levels of noise

Figure 1 shows the segmentation results of two synthetic images. The first one is an image with intensity inhomogeneity and the second one is contaminated by high levels of noise. From top to bottom, the results of the three rows show the performances of the CV model, LBF model and our model respectively. It is apparent that our model gets the similar correct segmentation results at iterations of 30 and 15 for the two images, whereas LBF model requires 60 and 40 iterations. For CV model, it costs up to 500 and 100 iterations for the images and still cannot get the correct results

Table 1

Iteration numbers of CV model, LBF model and our model

Figure	CV Model	LBF Model	Our Model
Figure 1(c)	500	60	30
Figure 1(f)	100	40	15
Figure 2(c)	10	10	5
Figure 2(e)	50	35	20
Figure 2(g)	55	130	30
Figure 3(c)	-	450	50
Figure 4(c)	500	110	90
Figure 4(f)	200	170	70
Figure 5(c)	300	50	30

because of the intensity inhomogeneity and high noise level. These experiments demonstrate that our model offers promising performance on synthetic images with intensity inhomogeneity or high levels of noise.

4.2. Synthetic images with different levels of noise

We make a series of experiments on synthetic images with different noise levels in Figure 2. From left to right, the images' noise levels get progressively higher. The results of the three rows show the performances of CV model, LBF model and our model respectively from top to bottom. We can observe that all three models get the correct segmentation results with very few iterations in column (c), while in columns (e) and (g), CV model fails to segment the two images with higher noise levels. Although LBF model can overcome the influence of high levels of noise and segment these two images, its values of iterations (35 and 130) are much higher than those (20 and 30) of our model. And as the noise level gets higher, we can also observe that the values of iterations of LBF model increase much faster than our model's. The results demonstrate that our model has excellent performance in terms of robustness to high levels of noise

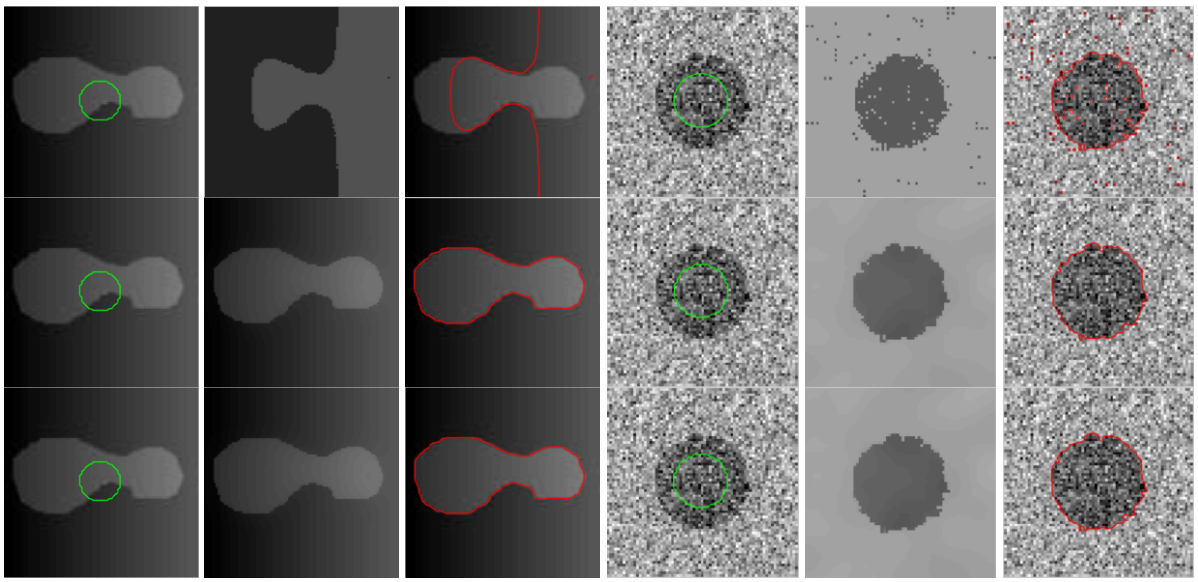

Fig. 1. Results for inhomogeneous and noisy synthetic images. Green contours and red contours represent the initial contours and final contours correspondingly. From top to bottom, the first row is the results of CV model at iterations of 500 (left) and 100 (right), the second row is the results of LBF model at iterations of 60 (left) and 40 (right), and the third row is the results of our model at iterations of 30 (left) and 15 (right). In each panel, columns (a) and (d) are initial contours, columns (b) and (e) are fitting images, and columns (c) and (f) are final results.

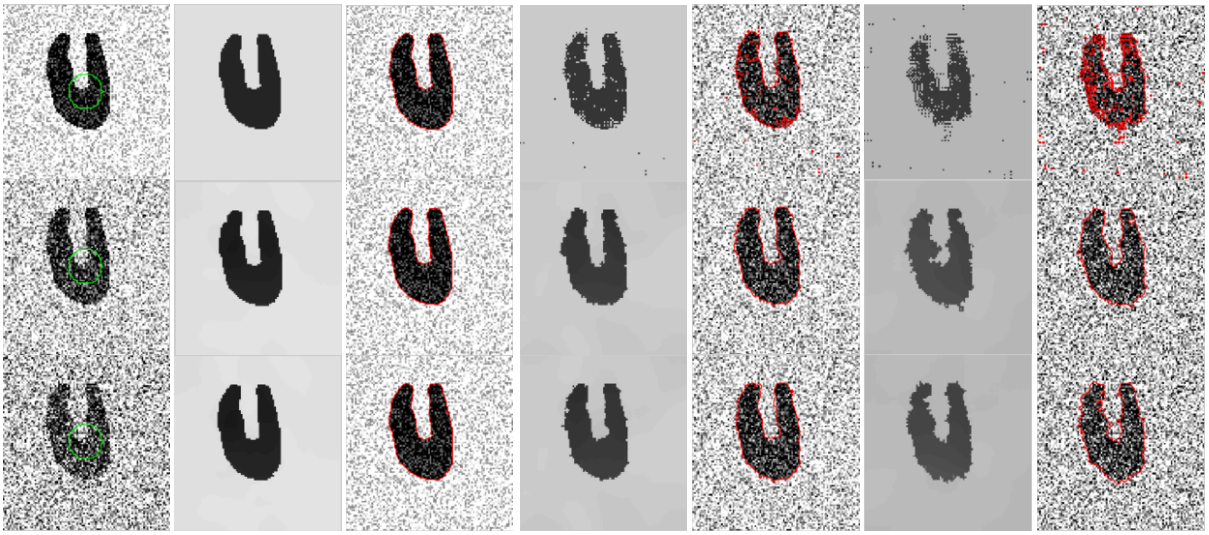

Fig. 2. Results for images with different noise levels. Green contours and red contours represent the initial contours and final contours correspondingly. From top to bottom, the first row is the results of CV model at iterations of 10 (left), 50 (middle) and 55 (right), the second row is the results of LBF model at iterations of 10 (left), 35 (middle) and 130 (right), and the third row is the results of our model at iterations of 5 (left), 20 (middle) and 30 (right). In each panel, column (a) is initial contours of three images, columns (b), (d) and (f) are fitting images, and columns (c), (e) and (g) are final results.

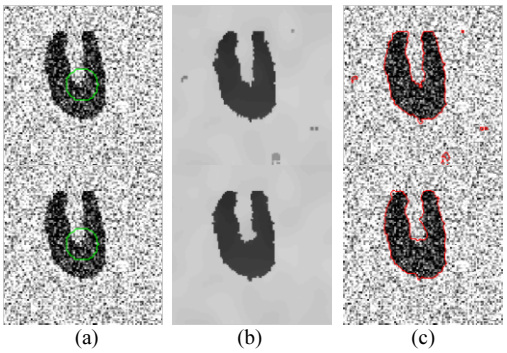

Fig. 3. Results for image with smaller neighborhood regions. Green contours and red contours represent the initial contours and final contours correspondingly. From top to bottom, the first row is the results of LBF model at iteration of 450, and the second row is the results of our model at iteration of 50. In each panel, column (a) is initial contours, column (b) is fitting images, and column (c) is final results.

4.3. Synthetic images with smaller neighborhood region

In Figure 3, we perform an image with smaller neighborhood region shown in column (g) of Figure 2 whose noise level is very high for both the LBF model (first row) and our model (second row). We can observe that our model still can succeed to segment the image with such high levels of noise and small neighborhood region in column (c) whereas the LBF model cannot get the correct segmentation result due to the lack of image information of a larger neighborhood region. Furthermore, our model costs only 50 iterations to segment the image successfully whereas LBF model fails to do so at 450

iterations. These results show that our model requires less computational power to perform well on images with smaller neighborhood regions.

4.4. Real images with intensity inhomogeneity/high levels of noise

Figure 4 shows the segmentation results of two real medical images. The first image is a heterogeneous medical vessel image and the second one is a liver image with high levels of noise. The results of the three rows are performances of CV model, LBF model and our model respectively from top to bottom. In columns (c) and (f), we can observe that CV model fails to segment the vessel image and liver image even at iterations of 500 and 200 due to the intensity inhomogeneity and noises, and that LBF model and our model can attain correct segmentations. However, our model can segment the images at iterations of 90 and 70 whereas LBF model requires iterations of 110 and 170. These results demonstrate the superior performance of our model for real medical images with intensity inhomogeneity or high levels of noises.

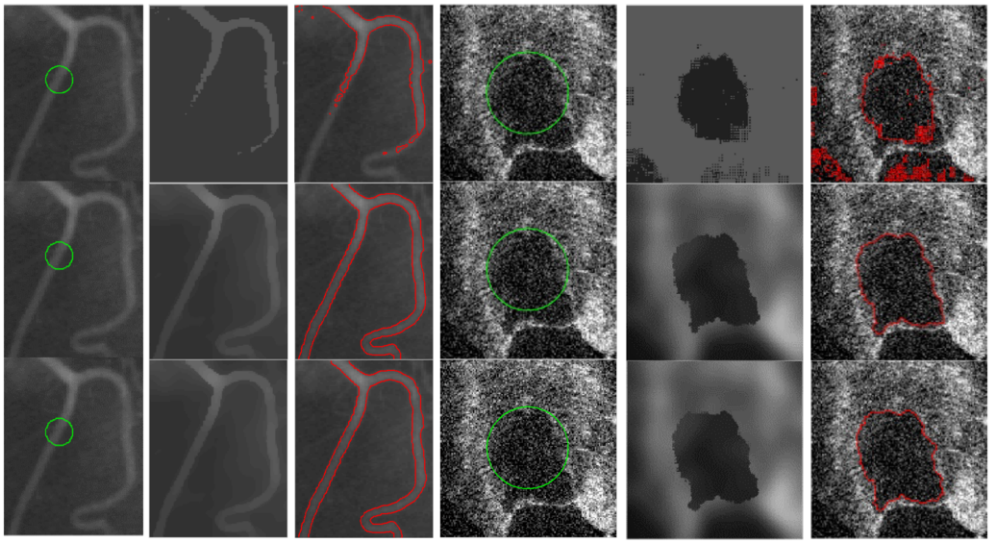

(a) (b) (c) (d) (e) (f)

Fig. 4. Results for inhomogeneous and noisy real medical images. Green contours and red contours represent the initial contours and final contours correspondingly. From top to bottom, the first row is the results of CV model at iterations of 500 (left) and 200 (right), the second row is the results of LBF model at iterations of 110 (left) and 170 (right), and the third row is the results of our model at iterations of 90 (left) and 70 (right). In each panel, columns (a) and (d) are initial contours, columns (b) and (e) are fitting images, and columns (c) and (f) are final results.

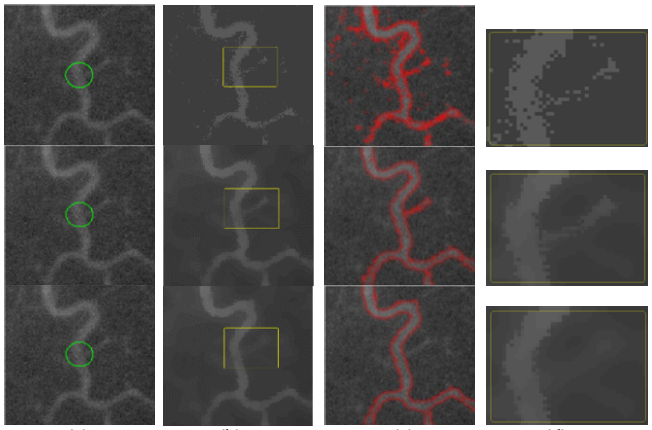

Fig. 5. Results for the image with intensity inhomogeneity and high levels of noise. Green contours and red contours represent the initial contours and final contours correspondingly. From top to bottom, the first row is the results of CV model at iteration of 300, the second row is the results of LBF model at iteration of 50, and the third row is the results of our model at iteration of 30. In each panel, column (a) is initial contours, column (b) is fitting images, column (c) is final results, and column (d) is middle rectangle of the image.

4.5. Real images with high levels of noise and intensity inhomogeneity

Figure 5 shows the segmentation results of a medical vessel image with intensity inhomogeneity and high levels of Gaussian noise. The results of the three rows are the performances of CV model, LBF model and our model respectively from top to bottom. We can observe that, in column (c) CV model cannot segment images even at high iterations (300), and LBF model fails to segment this image in the middle region marked by yellow rectangle at iteration of 50. If we carefully compare the fitting images of the three models in the yellow rectangle of column (d), we can observe remarkable differences that are quite important to the segmentation processes. As we know, LBF model is inevitably influenced by the Gaussian noise and intensity inhomogeneity, so it fails to fit the correct fitting image even at iteration of 300. With the correct fitting in the yellow rectangle, our model gets the correct segmentation result at a low iteration of 30. The results demonstrate our model's promising performance for images with high levels of noise and intensity inhomogeneity.

5. Conclusion

In this paper, we proposed a novel region-based level set model. After analyzing the traditional fitting operation of LBF model in the procedures of image domain fitting and energy domain fitting, we replaced the traditional GKFWS with median filter operation in the procedure of energy domain fitting. This makes the model robust to noises while better at retaining the original edge information. Furthermore, we incorporated the edge information into the segmentation process, which could further improve the performance of our model. Together, the experiments here demonstrate the promising performance of our model in terms of computational cost, robustness to noises and segmentation of images with intensity inhomogeneity.

Acknowledgement

This work is supported by the National Natural Science Foundation of China under Grant No. 61370133.

References

[1] J. Cheng, Y. C hou, C. Huang et al., ACCOMP: Augmented cell competition algorithm for breast lesion demarcation in sonography, Medical Physics **37** (2010), 6240–6252.
[2] F. Yeh, J. Cheng, Y. Chou et al., Stochastic region competition algorithm for Doppler sonography segmentation, Medical Physics **39** (2012), 2867–2876.
[3] M. Kass, A. Witkin and D. Terzopoulos, Snakes: Active contour models, International Journal of Computer Vision **1** (1987), 321–331.
[4] C. Xu, and J. Prince, Snakes, shapes and gradient vector flow, IEEE Transactions on Image Process **7** (1998), 359–369.
[5] L. Liu and A.C. Bovik, Active contours with neighborhood-extending and noise-smoothing gradient vector flow external force, EURASI P Journal on Image and Video Processing **2012** (2012), 9.
[6] V. Caselles, F. Catte, T. Coll and F. Dibos, A geometric model for active contours in image processing, Number Math. **66** (1993), 21–31.
[7] V. Caselles, R. Kimmel and G. Sapiro, Geodesic active contours, International Journal of Computer Vision **22** (1997), 61–79.
[8] T. Chan and L. Vese, Active contours without edges, IEEE Transactions on Image Processing **66** (2001), 266–277.
[9] C. Li, C. Kao, Gore, C. John and Z. Ding, Implicit active contours driven by local binary fitting energy, IEEE Conference on Computer Vision and Pattern Recognition, 2007, 1–7.
[10] X. Wang and M. Li, Level set model for image segmentation based on dual contour evolutional curve, Journal of Image and Graphics **19** (2014), 373–380.
[11] X. Wang, D. Huang and H. Xu, An efficient local chan-vese model for image segmentation, Pattern Recognition **43** (2010), 603–618.
[12] L. Liu, Q. Zhang, M. Wu and F. Shang, Adaptive segmentation of magnetic resonance images with intensity inhomogeneity using level set method, Magnetic Resonance Imaging **31** (2013), 567–574.
[13] L. Wang, C. Li, Q. Sun, D. Xia and C. Kao, Active contours driven by local and global intensity fitting energy with application to brain MR image segmentation, Computerized Medical Imaging and Graphics **33** (2009), 520–531.
[14] K. Zhang , H. Song and L. Zhang, Active contours driven by local image fitting energy, Pattern Recognition **43** (2010), 1199–1206.
[15] G.R. Reddy, D. Bochu, R. Kama and R. Rao, Standard median filtered bit–plane image segmentation using modified level sets, 2011 International Conference on Signal Processing, Communication, Computing and Networking Technologies, 2011, 30–35.
[16] D. Mumford and J. Shah, Optimal approximations by piecewise smooth functions and associated variational problems, Communications on Pure and Applied Mathematics **42** (1989), 577–685.
[17] C. Li, C. X, C. Gui and M.D. Fox, Level set evolution without re-initialization: A new variational formulation, Computer Vision and Pattern Recognition **1** (2005), 430–436.
[18] R. Yang, L. Yin, M. Gabbouj, J. Astola and Y. Neuvo, Optimal weighted median filters under structural constraints, IEEE Transactions on Signal Processing **43** (1995), 591–604.
[19] G.R. Arce, Median and weighted median smoothers, in: Nonlinear Signal Processing: A Statistical Approach, Wiley, New Jersey, 2005, pp. 81–136.